

Supporting Information

Cheng et al. 10.1073/pnas.1014186108

SI Text

Na⁺ Punch-Through Data Analysis. Na⁺-modified current voltage (IV) curves were fitted with Eq. S1 at intermediate voltages (25–150 mV), which describes the equilibrium block process for Na⁺ binding in the low-affinity cavity binding site (1).

$$I(V) = \frac{I_0(V)}{1 + \frac{[\text{Na}^+]}{K_B(0)e^{\frac{zV}{RT}}}}. \quad \text{[S1]}$$

$I_0(V)$ was obtained by fitting the control IV curve with an empirical function. The apparent affinity at 0 mV, $K_B(0)$, and voltage dependence, z , of the block were the fitted block parameters. All data fits were performed with Origin (Microcal).

In order to incorporate the subsequent rise in current at higher voltages into the model, we assume the cavity-bound Na⁺ can move either forward through the selectivity filter or back to the intracellular milieu and that the Na⁺ contribution to the current (when moving forward through the filter) is insignificant relative to K⁺, as verified by replacing K⁺ with Na⁺ on the intracellular side. The entire Na⁺ block IV curve can then be fit by assuming a model (Scheme S1) where the vestibule (V) can be occupied by either a Na⁺ or a K⁺ and that both ions can dissociate either back toward the intracellular solution (b_{-1} for Na⁺, negligible for K⁺ at high voltages where punch through becomes visible), or forward through the selectivity filter (b_2 for Na⁺, k_2 for K⁺). Consequently, current through the channel will be described by Eq. S2, derivation of which is detailed in Nimigean and Miller (2):

$$I(V) = I_0(V) \left(1 + \frac{[\text{Na}^+]}{(1 + \frac{[\text{K}^+]}{k_2/k_1})(b_{-1}/b_1 + b_2/b_1)} \right)^{-1}, \quad \text{[S2]}$$

where k_1 and b_1 are the on rates for K⁺ and Na⁺ binding to the cavity, k_2 and b_2 are the rates of K⁺ and Na⁺ expulsion through the selectivity filter, and b_{-1} is the off rate of dissociating back to the intracellular milieu. Fits of Eq. S2 will yield values for the “punch-through” constant, b_2/b_1 , the Michaelis-type constant for K⁺, k_2/k_1 , and the equilibrium block parameter b_{-1}/b_1 . Under conditions of high voltage such that the expulsion of Na⁺ toward the outside is much faster than its dissociation toward the intracellular milieu, Eq. S2 can be modified to calculate a lower limit on k_2/b_2 , a measure of the number of K⁺ ions exiting the channel per Na⁺ ion (2).

$$k_2/b_2 \geq \left(\frac{I_0}{I} - 1 \right) \left(\frac{[\text{K}^+]}{[\text{Na}^+]} \right) \left(\frac{k_1}{b_1} \right) \left(1 + \frac{k_2/k_1}{[\text{K}^+]} \right), \quad \text{[S3]}$$

where k_2/k_1 is set to 0 in order to obtain a lower limit and k_1/b_1 to 2.5, the same value as for WT (2). The justification for using the same value of k_1/b_1 as in WT is our finding (see text) that the equilibrium Na⁺ block in E71A displays similar parameters [$K_B(0)$, z] as the WT channel. An extended description of this analysis can be found in ref. 2.

Reversal Potential Measurements Lack the Sensitivity to Detect Small Changes in Selectivity in This Case. The suggestion of Cordero-Morales et al. (3) that K⁺ selectivity is increased in the E71A channel was based on extrapolated reversal potentials in biionic conditions, also known as vanishing current measurements (200 mM Na⁺ inside and 200 mM K⁺ outside). Given the lack of any

measurable Na⁺ currents, and the fact that KcsA channels are predominantly blocked by high concentrations of intracellular Na⁺ (2, 4), conclusions about permeability ratios extracted from these measurements must be taken tentatively. We repeated these experiments by measuring reversal potential shifts with intracellular K⁺ and varying concentrations of extracellular (pipette) K⁺ and Na⁺ chosen to maintain equal ionic strength across the membrane (Fig. S3A). Under these conditions, E71A reversal potentials are statistically not different from WT (Fig. S3B). Both E71A and WT reversal potential shifts with varying K⁺ and no Na⁺ (Fig. S3B, black diamonds) are significantly different from pure K⁺ selectivity (black line) and surprisingly close to the values obtained with Na⁺, indicating that such measurements with Na⁺ are approaching the limit of the analysis. Indeed, a more sensitive strategy using comparative analysis with the highly selective ionophore, valinomycin, was needed to achieve a more accurate estimate of selectivity in KcsA (4). We propose that, in the presence of K⁺, E71A exhibits a small reduction in selectivity that is detectable in the more sensitive flux assays (Fig. 3) and a Na⁺ blocker punch-through experiment (Fig. 4), but not reversal potential measurements. The flux assay is sensitive enough to detect differences in permeation between two ions whose conductivities are too small to yield measurable currents

Structure Validation. Because of the low resolution of the crystallographic data for the E71A KcsA in the absence of K⁺, we took precautions to verify that the final model (shown in Fig. 5A) was not inadvertently biased by the molecular replacement (MR) starting model. We ran multiple molecular replacement jobs using different starting models, in which the selectivity filter was arranged in different conformations. These models included the wild type, high K⁺ structure (PDB ID code 1K4C), the low K⁺ “collapsed” structure (PDB ID code 1K4D), and the “flipped” structure (PDB ID code 2ATK). Fig. S4 demonstrates the initial maps generated immediately following molecular replacement with these starting models. Fig. S4A shows the initial 2Fo-Fc and Fo-Fc maps following MR with the nonflipped, non-collapsed starting model 1K4C (the high K⁺ KcsA structure in ref. 5). The 2Fo-Fc map is disrupted from residue V81 through Y78, and negative Fo-Fc density surrounds D80, suggesting that the aspartate is not correctly positioned. Fig. S4B depicts the initial 2Fo-Fc and Fo-Fc maps following MR with the nonflipped, collapsed starting model 1K4D (the low K⁺ KcsA structure in ref. 5). The 2Fo-Fc map is even further disrupted along the entire selectivity filter, and negative Fo-Fc density is observed around D80 (again suggesting that the aspartate is modeled incorrectly) and the selectivity filter backbone (suggesting that the conformation of the selectivity filter is different). In contrast, Fig. S4C reveals that the initial model derived from MR using the flipped, noncollapsed starting model 2ATK (the flipped E71A KcsA structure from ref. 3) provides the best fit to the initial density. Further rounds of map-supported manual manipulation and refinement resulted in all of the models having nearly identical selectivity filters, similar to that observed in the flipped structure, 2ATK. The structure presented in this study was generated using 2ATK as a starting model due to the final residual values being slightly less than those generated using other starting models, although the final structures and maps were very similar. In addition, Fig. S5 demonstrates the close agreement of our final model with an annealed omit map generated in CNS (residues 69–81 removed from map calculation). Ultimately, we chose to use 2ATK as the starting model because the residual values were

lower and the final map better, despite the final differences being minimal. These maps strongly support the conformation of the filter in our structure model and show that it is not biased by the initial model used for the molecular replacement.

Liquid Junction Potentials. The following steps were taken to account for or determine offsetting and liquid junction potentials when measuring reversal potentials. We ensured that the ground electrode in the bath always “saw” the same solution as that in the pipette to prevent any offsetting potential between the pipette and ground electrodes. Before sealing onto a liposome, the pipette was inserted into the reference solution (i.e., 154 mM

KCl) in the bath, and with the amplifier in current clamp set to zero current, the offset was then manually adjusted to read zero voltage. Liquid junction potentials were then measured by moving the pipette from the reference into the test solution (e.g., from 154 mM KCl to 120 mM NaCl + 34 mM KCl) and measuring the resultant change in voltage. We found for all test solutions that the liquid junction potentials were small (<1 mV) and correction of the data was not necessary. Also, a small junction potential would not alter our conclusion from the reversal potential measurements: that no difference can be detected between WT and E71A.

1. Woodhull AM (1973) Ionic blockage of sodium channels in nerve. *J Gen Physiol* 61:687–708.
2. Nimigean CM, Miller C (2002) Na⁺ block and permeation in a K⁺ channel of known structure. *J Gen Physiol* 120:323–335.
3. Cordero-Morales JF, et al. (2006) Molecular determinants of gating at the potassium-channel selectivity filter. *Nat Struct Mol Biol* 13:311–318.

4. LeMasurier M, Heginbotham L, Miller C (2001) KcsA: It's a potassium channel. *J Gen Physiol* 118:303–314.
5. Zhou Y, Morais-Cabral JH, Kaufman A, MacKinnon R (2001) Chemistry of ion coordination and hydration revealed by a K⁺ channel-Fab complex at 2.0 Å resolution. *Nature* 414:43–48.

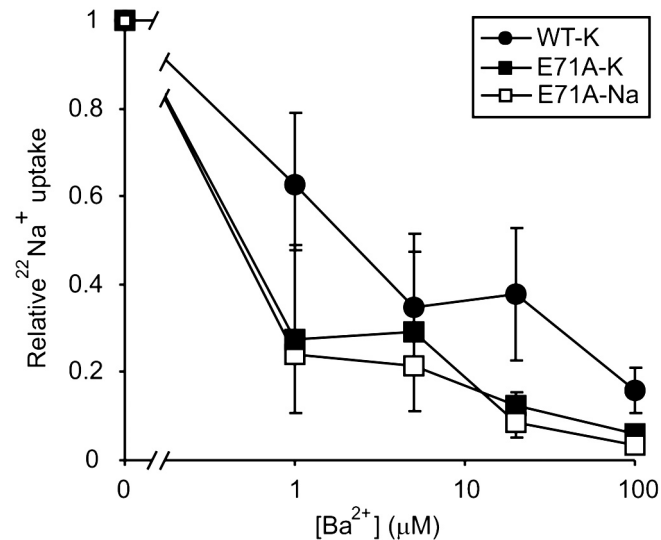


Fig. S1. Ba²⁺ sensitivity of K⁺ and Na⁺-driven ²²Na⁺ fluxes in E71A KcsA, and Na⁺-driven ²²Na⁺ fluxes in WT KcsA. Na⁺-driven fluxes through E71A exhibit similar Ba²⁺ sensitivity as K⁺-driven fluxes. Each data series is normalized to ²²Na⁺ counts in the absence of Ba²⁺ (n = 3, mean ± SEM).

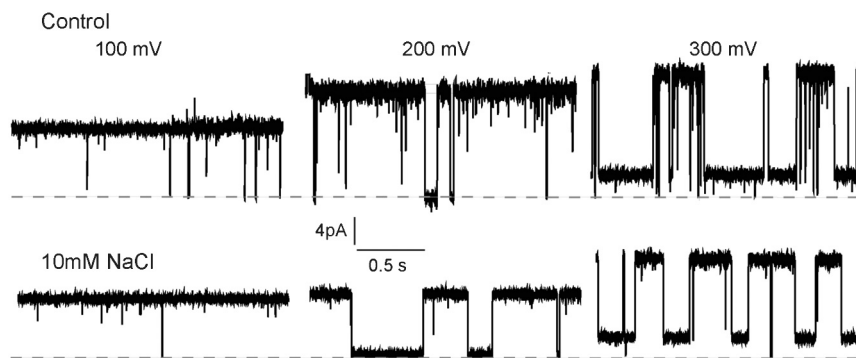


Fig. S2. Representative traces from single channel recordings of E71A KcsA currents with or without the presence of 10 mM NaCl at 100, 200, and 300 mV. Dashed line represents the zero current level. There is a highly reproducible voltage-dependent subconductance level in the E71A KcsA channel that becomes prevalent at voltages higher than 200 mV in both the control and the Na⁺-modified currents that we did not investigate in detail.

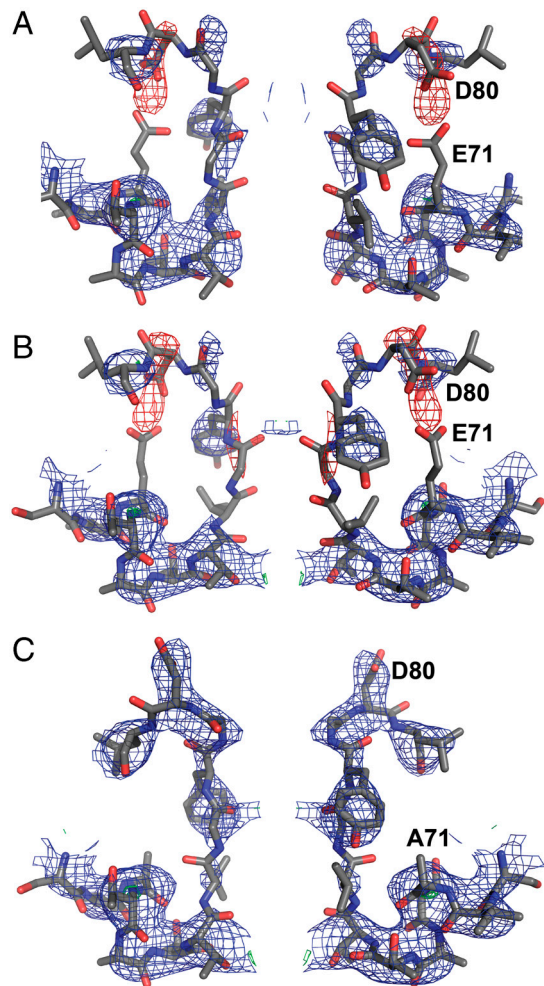


Fig. 54. Selectivity filters for the E71A KcsA in the absence of K^+ and 1.2σ $2Fo-Fc$ (blue) and 3σ $Fo-Fc$ (positive green, negative red) maps following molecular replacement with (A) starting model PDB ID code 1K4C (nonflipped, noncollapsed), (B) starting model PDB ID code 1K4D (nonflipped, collapsed), and (C) starting model PDB ID code 2ATK (flipped, noncollapsed).

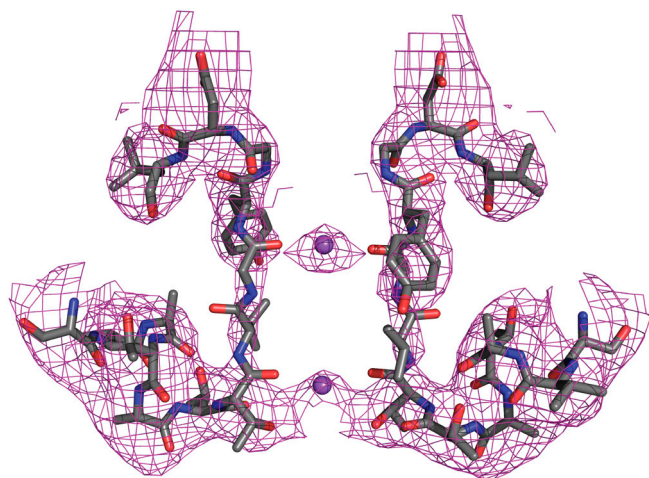


Fig. 55. Selectivity filter of E71A KcsA in the absence of K^+ with 1.2σ $Fo-Fc$ annealed omit map generated in CNS (residues 69–81 and Na^+ ions were removed from map calculation).

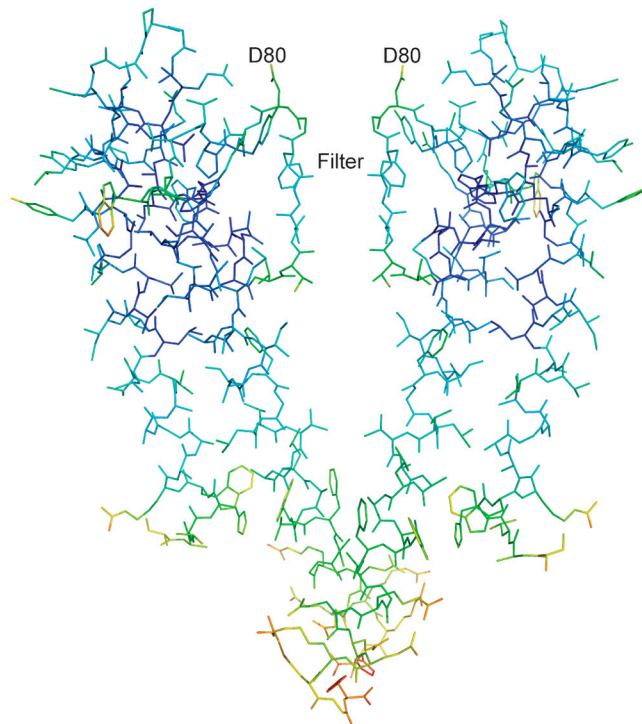


Fig. S6. Dimer of E71A KcsA in the absence of K^+ colored according to relative temperature factor (red high, blue low). The temperature factors in the selectivity filter region do not suggest particularly higher flexibility than the rest of the structure.

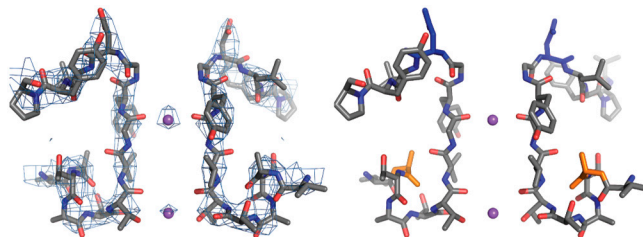


Fig. S7. Crystal structure of E71A KcsA in the presence of 2 mM K^+ and 148 mM Na^+ also features a flipped, noncollapsed selectivity filter similar to that observed in the absence of K^+ (Fig. 5A). The filter of the E71A crystal structure is presented as a stick model with Na^+ ions represented as purple spheres. The accompanying electron density ($2F_o - F_c$) is contoured at 1.0σ . Protein was prepared as described in *Materials and Methods* except for being dialyzed in 148 mM NaCl, 2 mM KCl, and 10 mM Tris pH 7.5. Crystallographic statistics are recorded in Table S1.

